Low Obstacle Avoidance for Lower Limb Exoskeletons

Edoardo Trombin[1], Stefano Tortora[1,2], Francesco Bettella[2], Alessandra Del Felice[2,3], Luca Tonin[1,2] and Emanuele Menegatti[1,2]

[1]Department of Information Engineering, University of Padova, 6b G. Gradenigo, Padova, 35131, Italy
[2]Padova Neuroscience Center, University of Padova, 2 G. Orus, Padova, 35131, Italy
[3]Department of Neuroscience, University of Padova, 160 Belzoni, Padova, 35131, Italy

Abstract

Powered lower limb exoskeletons (LLEs) are innovative wearable robots that allow independent walking in people with severe gait impairments. Despite the recent advancements, the use of this promising technology is still restricted to clinical settings; uptake in real-life conditions as a device to promote user independence is still lacking due to the difficulty of controlling these devices in unstructured and complex environments. In this work, we propose a vision-assisted method for low obstacle avoidance to enhance the autonomy of LLEs. The exoskeleton collects information from the surroundings through a RGB-D camera to recognize and segment objects on the ground that might affect the walking pattern. Then, the method identifies suitable foothold positions. In addition, a novel iterative gait trajectory generator is proposed to automatically compute collision-free walking paths. We believe that re-thinking exoskeletons as semi-autonomous agents will represent not only the cornerstone to promote a more symbiotic human-exoskeleton interaction but may also pave the way for the use of this technology in the everyday life.

Keywords

Lower Limbs Exoskeletons, Assistive Robotics, Computer Vision, Obstacle Avoidance

1. Introduction

Powered lower-limb exoskeletons (LLEs) represent a recent assistive technology to allow people with gait impairment to regain the capability of walking [1]. The interest in this technology is not limited to the research community but is gaining attention from a commercial perspective: several exoskeletons are already available on the market (e.g., HAL [2], MindWalker [3]). However, the use of powered exoskeletons is still restricted to clinical settings or to highly controlled environments [4]. Indeed, LLEs generate pre-programmed walking patterns which are repeated all alike or—at most—implement gait patterns individualized for each user [5]. The research community has tried to face this limitation by implementing pre-defined locomotion modes for ground-walking, inclined planes, stair walking [6]. However, the user is often required to manually switch between the different modes [7] and a run-time estimation of the robot's gait control parameters for adapting the walking to the specific environmental obstacles (e.g., objects on the ground) is generally not considered. In unstructured real-world settings, this can be inconvenient and cognitively demanding as the control burden is entirely on the user. To

AIRO 2022: 9th Italian Workshop on Artificial Intelligence and Robotics, November 30 2022 Udine, Italy
edoardo.trombin@studenti.unipd.it (E. Trombin); stefano.tortora@unipd.it (S. Tortora)

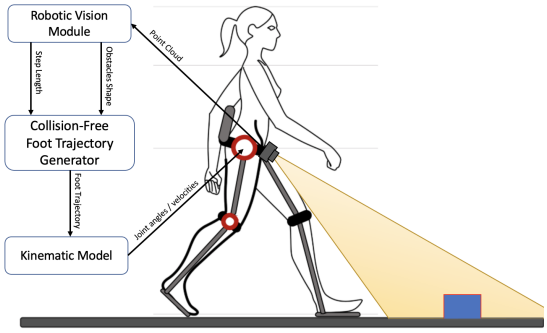

Figure 1: Pipeline of the proposed method

overcome these limitations, we propose a novel vision-based control approach for low-obstacle avoidance in lower-limb exoskeletons. The proposed method is schematically displayed in Figure 1. A RGB-D camera is mounted on the exoskeleton pelvis and a Robotic Vision module is implemented for detecting ground plane and obstacles, and compute the next foothold position taking into consideration robot state, obstacles' shape and safety constraints. In addition, a novel iterative-based Collision-Free Foot Trajectory Generator (CFFTG) and a parameterized gait kinematic model are proposed to compute hip and knee joints' angles that are sent to the robot PID controller to produce a feasible gait pattern allowing to avoid the detected obstacles. Our preliminary results in a simulation experiment show that the proposed autonomous gait planning method allows the exoskeleton to successfully perform a step in complex walking conditions without collisions.

2. Methods

2.1. Robotic Vision Module

The Robotic Vision module takes the data from the RGB-D camera to perceive the environment in order to recognize the spatial position and geometric shape of the obstacles that may interfere with the walking. First, the point cloud is aligned with the robot coordinate frame through an homogeneous transformation. Then, the ground plane is identified using the RANSAC algorithm [8] and separated from the input point cloud. The remaining points of the cloud are labelled as obstacle points. Rectangular area in front of each foot, with dimension [foot width × maximum step length] is considered (Figure 2(a)). For each point within this area, a score is computed taking into consideration: (i) presence of an obstacle point, to which a score of 0 is immediately applied; (ii) linear distance to the closest obstacle point; (iii) average step length, to privilege a consistent step cadence, as shown in Figure 2(b). In case no obstacle is detected, only the average step length is automatically considered. Finally, a sliding window is applied to each area (i.e., the window will have the dimension of the foot) to find the region in which the mean score of the points in the window is maximised. If a window contains a point whose score is 0, the whole window is discarded. If a feasible window is found, the step length is computed

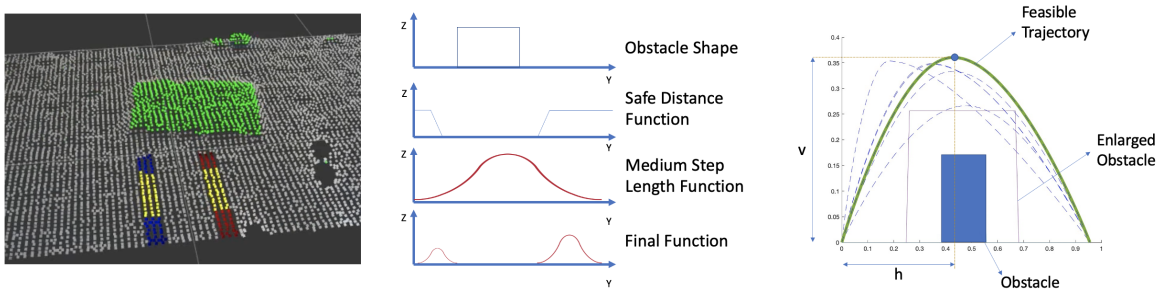

Figure 2: (a) Visualisation of the output produced by the Robotic Vision Module, along with the proposed next step position (highlighted in yellow). (b) Functions used to compute the score for each track point. (c) Visualisation of the CFFTG algorithm's iterations.

considering the center of the window.

2.2. Collision-Free Foot Trajectory Generator (CFFTG)

After having predicted the next foothold, a CFFTG algorithm is in charge of producing the foot trajectory that doesn't collide with the identified obstacles. In practice, the gait trajectory is modelled as a cubic polynomial curve that has its starting point in the current foot position and its final point in the center of the foothold found by the Robotic Vision module. Fixing the start and end points, the curve has two degrees of freedom, which are the horizontal h and vertical v position of the foot trajectory peak. To identify these parameters, a randomized iterative state-space search [9] is exploited. In particular, h and v are firstly initialized using gaussian random variables with means equal to half the step length and to average step height, respectively. If the trajectory resulting from the current h and v parameters doesn't collide with obstacle, it is returned in output; otherwise, the minimum euclidean distance between the trajectory and the obstacle is computed. Also, new values for h and v are generated from the gaussian random variables. If the newly computed trajectory is still in collision but its minimum distance to obstacle is higher than the previous one, the means of the random variables are set to the current values of h and v and the variances are reduced by a scale factor to restrict the search space. This trajectory generation process is iterated until a feasible trajectory is found or the maximum number of iterations is reached. In the second case, the process is repeated with a different initialization of the random variables to account for the presence of local minima in the searching process. An example of the CFFTG iterations is shown in Figure 2(c).

This motion planning algorithm has been implemented as it results in smooth foot trajectories similar to the physiological walking pattern [10] and since it is shown to converge faster to a feasible solution than other motion planning algorithms [11]. This aspect is fundamental in walking applications as the exoskeleton should predict and elaborate the next step motion during the stance phase, which lasts about 400 ms in able-bodied locomotion.

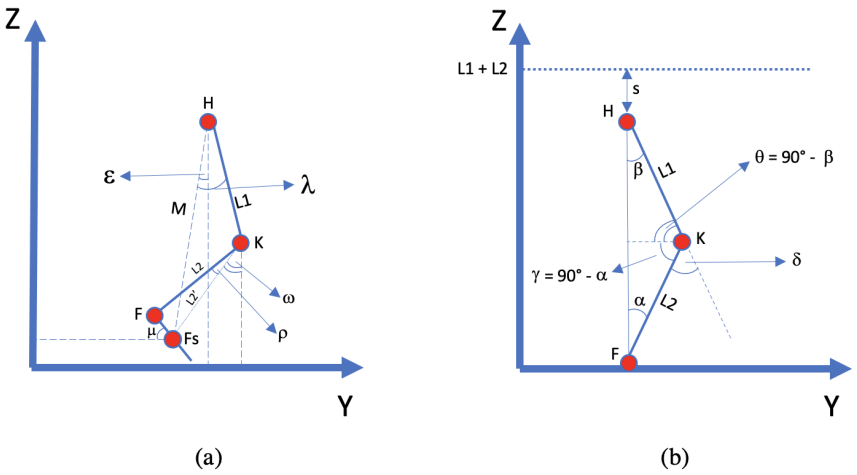

Figure 3: Kinematic model of the swing leg (a) and single-support leg (b) in the sagittal plane

2.3. Parameterized Kinematic Model

A parameterized kinematic model is implemented to achieve a run-time adaptation of the gait pattern according to the outcome of the CFFTG algorithm. The employed kinematic model is shown in Figure 3 (a) for the swing leg, and in Figure 3 (b) for the single-support leg. The model has two active degrees of freedom at the hip and knee joints, while the passive ankle joint is assumed to be fixed at 90° during the swing phase, and compliant during the stance phase, to keep the foot parallel to the ground. Based on the bio-mechanical literature [12], the motion of the center of mass (CoM) during the swing phase is shown to follow a cubic polynomial curve in the vertical direction that has its minimum when the swing leg is parallel to the single-support leg, that is flexed of $\delta \simeq 20^\circ$ for a better support. To calculate this vertical translation s, we exploited the crank-connecting rod mechanism [13] (see Figure 3 (b)):

$$s = L_1 + L_2 - (L_1 \cdot \cos(\beta) + L_2 \cdot \cos(\alpha)) \tag{1}$$

Finally, knowing the full CoM and foot trajectories and given the leg length constraints, the trajectory of each active joint can be retrieved from the inverse kinematic solution:

$$\theta_H = \arctan(\frac{H_z - K_z}{K_y - H_y}) \tag{2}$$

$$\theta_K = \theta_H - \arctan(\frac{K_z - F_z}{F_y - K_y}) \tag{3}$$

3. Experiments & Results

Six experiments have been carried out by simulating a situation where the LLE was challenged to surpass different obstacles: following a hardware-in-the-loop approach, point clouds were acquired with a RealSense D-455 Stereo Camera to test the Robotic Vision module on real data,

Table 1
Means and standard deviations of notable experimental values

Value	Mean
Obstacle Detection Error	0.35 cm ± 0.25 cm
RV execution time	61.48 ms ± 20.45 ms
CFFTG execution time	20.35 ms ± 5.73 ms

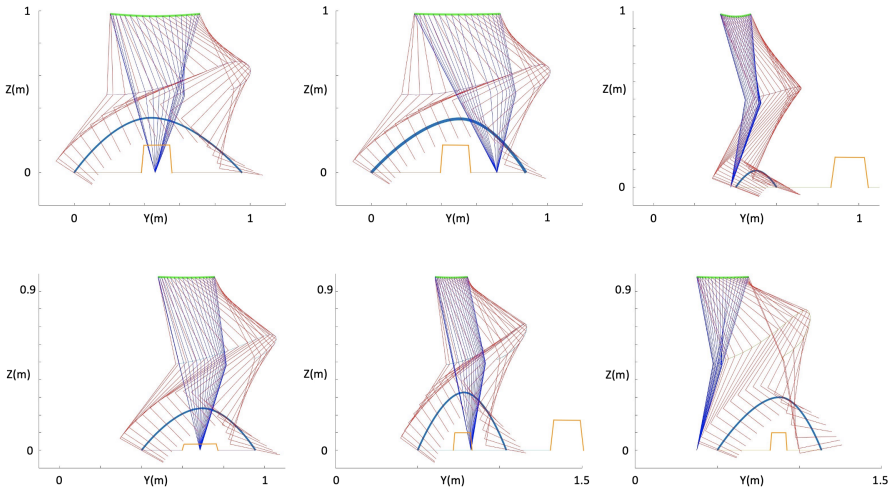

Figure 4: Kinematic simulation results for the six experiments. The elements depicted are: foot trajectory (dark blue), single support leg (blue), leg executing the step (red), obstacle (orange), hip trajectory (green).

and based on the detection a simulated version of the environment was produced to test CFFTG and kinematics. It is worth noting that we assumed perfect obstacles tracking with respect to the exoskeleton reference frame since experiments have been conducted in a simulated environment. Visuo-inertial SLAM techniques [14] will be considered as soon as the system will be implemented and evaluated on a real LLE. Table 1 shows the parameters monitored during the experiments. Figure 4 shows the outcome of the CFFTG algorithm and kinematic model for the six experiments. In all the conditions, the method was able to produce a feasible gait pattern avoiding collisions with obstacles of different shapes and height with suitable computational time.

4. Conclusions & Future Work

This work presents a new vision-based method to control LLEs with the aim of increasing the autonomy of these devices in real-world applications. Future work will focus on implementing and testing this approach on a real exoskeleton, as well as new approaches will be considered for the vision module in order to extend it to be used in outdoor settings.

Acknowledgments

ST is supported by the Department of Information Engineering, Univ. of Padova, under the HyDRA-Walker project. FB is supported by Italian Minister for Education (MUR), under REACT-EU PON "Ricerca e Innovazione". LT is supported by the Department of Information Engineering, Univ. of Padova, under the BrainGear project (TONI_BIRD2020_01).

References

[1] D. Pinto-Fernandez, D. Torricelli, M. del Carmen Sanchez-Villamanan, F. Aller, K. Mombaur, R. Conti, N. Vitiello, J. C. Moreno, J. L. Pons, Performance evaluation of lower limb exoskeletons: a systematic review, IEEE Transactions on Neural Systems and Rehabilitation Engineering 28 (2020) 1573–1583.

[2] A. Tsukahara, Y. Hasegawa, K. Eguchi, Y. Sankai, Restoration of gait for spinal cord injury patients using hal with intention estimator for preferable swing speed, IEEE Transactions on neural systems and rehabilitation engineering 23 (2014) 308–318.

[3] S. Wang, L. Wang, C. Meijneke, E. Van Asseldonk, T. Hoellinger, G. Cheron, Y. Ivanenko, V. La Scaleia, F. Sylos-Labini, M. Molinari, et al., Design and control of the mindwalker exoskeleton, IEEE transactions on neural systems and rehabilitation engineering 23 (2014) 277–286.

[4] O. Lennon, M. Tonellato, A. Del Felice, R. Di Marco, C. Fingleton, A. Korik, E. Guanziroli, F. Molteni, C. Guger, R. Otner, et al., A systematic review establishing the current state-of-the-art, the limitations, and the desired checklist in studies of direct neural interfacing with robotic gait devices in stroke rehabilitation, Frontiers in Neuroscience 14 (2020) 578.

[5] Z. Zhou, B. Liang, G. Huang, B. Liu, J. Nong, L. Xie, Individualized gait generation for rehabilitation robots based on recurrent neural networks, IEEE Transactions on Neural Systems and Rehabilitation Engineering 29 (2020) 273–281.

[6] S. S. P. A. Bishe, T. Nguyen, Y. Fang, Z. F. Lerner, Adaptive ankle exoskeleton control: Validation across diverse walking conditions, IEEE Transactions on Medical Robotics and Bionics 3 (2021) 801–812.

[7] S. O. Schrade, K. Dätwyler, M. Stücheli, K. Studer, D.-A. Türk, M. Meboldt, R. Gassert, O. Lambercy, Development of varileg, an exoskeleton with variable stiffness actuation: first results and user evaluation from the cybathlon 2016, Journal of neuroengineering and rehabilitation 15 (2018) 1–18.

[8] K. G. Derpanis, Overview of the ransac algorithm, Image Rochester NY 4 (2010) 2–3.

[9] H. H. Hoos, E. Tsang, Chapter 5 - local search methods, in: F. Rossi, P. van Beek, T. Walsh (Eds.), Handbook of Constraint Programming, volume 2 of *Foundations of Artificial Intelligence*, Elsevier, 2006, pp. 135–167. URL: https://www.sciencedirect.com/science/article/pii/S157465260680009X. doi:https://doi.org/10.1016/S1574-6526(06)80009-X.

[10] L.-S. Chou, K. R. Kaufman, R. H. Brey, L. F. Draganich, Motion of the whole body's center of mass when stepping over obstacles of different heights, Gait & Posture 13 (2001) 17–26.

[11] K. Balakrishana Reddy, G. Suresh, R. K. Mandava, A. Kumar, T. Ch, A short review on biped

robots motion planning and trajectory design, Advancement in Materials, Manufacturing and Energy Engineering, Vol. II (2022) 471–480.

[12] J. Carpentier, M. Benallegue, J.-P. Laumond, On the centre of mass motion in human walking, International Journal of Automation and Computing 14 (2017) 542–551. doi:10.1007/s11633-017-1088-5.

[13] F. Lisheng, T. Qingjun, Crank-connecting rod mechanism: its applications in ancient china and its origin, in: International symposium on history of machines and mechanisms, Springer, 2009, pp. 235–250.

[14] G. Oriolo, A. Paolillo, L. Rosa, M. Vendittelli, Humanoid odometric localization integrating kinematic, inertial and visual information, Autonomous Robots 40 (2016) 867–879.